Inference of ventricular activation properties from twelve-lead electrocardiogram

Julia Camps[1], Brodie Lawson[2], Christopher Drovandi[2], Ana Minchole[1], Zhinuo Jenny Wang[1], Vicente Grau[1], Kevin Burrage[1,2], Blanca Rodriguez[1]

[1]University of Oxford, Oxford, United Kingdom
[2]Queensland University of Technology, Brisbane, Australia

Abstract

The integration of cardiac magnetic resonance (CMR) imaging and electrocardiogram (ECG) data through advanced computational methods could enable the development of the cardiac 'digital twin', a comprehensive virtual tool that mechanistically reveals a patient's heart condition from clinical data and simulates treatment outcomes. The adoption of cardiac digital twins requires the non-invasive efficient personalisation of the electrophysiological properties in cardiac models. This study develops and evaluates new computational techniques to estimate key ventricular activation properties for individual subjects by exploiting the synergy between CMR, ECG, and modelling and simulation. We present an efficient sequential Monte Carlo approximate Bayesian computation-based inference method, integrated with Eikonal simulations and torso-biventricular models constructed based on clinical CMR imaging to recover conduction speeds and earliest activation sites from 12-lead ECGs. We demonstrate successful results of our inference method on a cohort of twenty virtual subjects with cardiac ventricular myocardial-mass volumes ranging from 74 cm³ to 171 cm³.

1.   Introduction

Recent studies have shown the power of patient-specific image-based modelling and simulation for therapy guidance, arrhythmic biomarkers interpretation and patient's phenotypic variability interpretation [1], [2]. This technology has paved the way towards realising the 'digital twin' vision [3], referring to a comprehensive virtual tool that coherently integrates a patient's clinical data with mechanistic physiological knowledge and informs therapeutic and diagnostic decision-making through simulations. Generating cardiac digital twins requires estimating patient-specific properties from clinical data.

We investigate new techniques for quantifying subject-specific ventricular activation properties using CMR-based torso-biventricular modelling and simulation and 12-lead ECG recordings. We present a 12-lead ECG-QRS-guided inference method combined with fast Eikonal simulations to determine the accuracy in estimating the conduction speeds and earliest activation sites (root nodes) as these properties determine the activation sequence in the ventricles [4]. We implement a sequential Monte Carlo approximate Bayesian computation (SMC-ABC) [5] based inference method and a dynamic time warping (DTW) based QRS distance metric. We evaluate our methods on a cohort of twenty virtual subjects from four anatomies.

2.   Materials and Methods

2.1.   Virtual subjects and simulations

We generated twenty virtual subjects by combining four biventricular geometries with myocardial-mass volumes ranging from 74 cm³ to 171 cm³ [6] and five conduction speeds (Table 1).

Table 1. Five conduction-speed (cm/s) configurations considered [6]. Abbreviations: endo – endocardial speed; myo – myocardial speeds (fibre, sheet, and sheet-normal).

Configuration name	Endo	Fibre	Sheet	Sheet-normal
Normal speeds	150	50	32	29
Slow endo	120	50	32	32
Fast endo	179	50	32	32
Fast endo & myo	179	88	49	45
Slow endo, fast myo	120	88	49	45

We simulated the 12-lead ECGs for these virtual subjects using CMR-based torso-biventricular Eikonal models solved as shortest path-finding problems [7] paired with the pseudo-ECG algorithm [8] for our 12-lead ECG simulations. Considering virtual subjects allowed knowing the ground truth to evaluate the inference, as in [9]. We contaminated the target ECGs with white Gaussian noise to reach 20 decibels of signal-to-noise ratio.

Our models implemented rule-based fibre orientations [10], orthotropic myocardial conduction speeds [11], isotropic endocardial speed, and root nodes, as in [9].
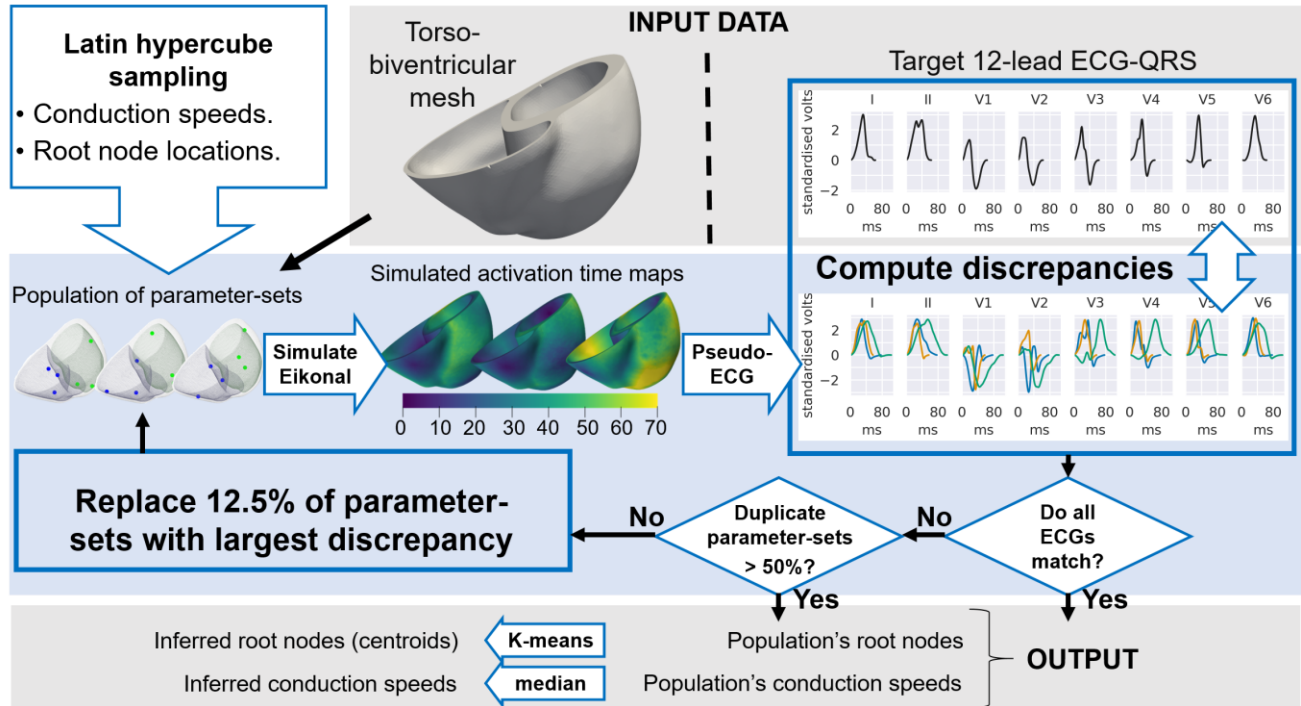
Figure 1. Proposed SMC-ABC based inference method. The process starts using Latin hypercube sampling (top-left) to generate a population of 512 Eikonal models with the same subject-specific CMR-based torso-biventricular mesh but different parameter values. During the iterative part of the algorithm, each model simulates its activation map, from which the pseudo-ECG algorithm computes the 12-lead ECG-QRS signals. Then, the discrepancy between each prediction and the target QRS complexes are computed and tested against the stopping criteria. If neither stopping criteria were met, the method would replace each parameter set within the top 12.5% discrepancies in the population by either a copy or mutation of another parameter-set with a discrepancy lower than the top 12.5%. Otherwise, upon the termination of the iterative process, the method outputs the centroids of the inferred root nodes and the median value of each inferred speed.

2.2.   Inference pipeline

We present an SMC-ABC-based method (Figure 1) to infer the human ventricular activation properties, namely, fibre, sheet (transmural) and sheet-normal fibre-oriented speeds, endocardial speed, and root nodes.

This inference process (Figure 1) searches for a population of models (with different parameter-sets but the same equations and subject-specific anatomical models) that yield 12-lead QRS simulations in agreement with the virtual subject's QRS. This agreement was measured with a DTW-based discrepancy metric that implements a warping-slope and parallelogram constraints [12], [13] to physiologically compare different QRS complexes.

This search is conducted in a parameter space representing the four conduction speeds (endocardial, fibre, sheet, and sheet-normal speeds) and the number and locations of the root nodes. While the conduction speeds can be represented as continuous values (constrained to physiological ranges [14]), the root nodes can change in number and position throughout the 3D biventricular endocardial surface. Thus, we discretised the root node parameter space to the centres of each endocardial segment according to the American Heart Association's segmentation guidelines [15], while ensuring that any point in either ventricle's endocardia had at least one root node in the same ventricle not more than 2.5 cm away. This selection strategy led to about 30 candidate locations per heart, from which between six to ten could be 'in use', following the findings in [4] on seven root nodes being enough to simulate realistic healthy 12-lead ECG signals.

These candidate root node locations were considered a binary parameter, with the inference yielding 'in use' or 'not in use' to obtain a good match between simulated and target QRS signal.

The navigation of this parameter space was conducted using an SMC-ABC algorithm. SMC-ABC uses a population of models with different parameter sets that represent the parameter search space of interest. The method then shrinks this parameter space of interest at each iteration, emphasising the 'promising regions'. This resampling is done by replacing the highest (12.5%) discrepancy parameter sets with mutations or copies of low discrepancy parameter sets.

The code of the inference pipeline can be found in

3.   Results

Our inference pipeline reproduced the standardised QRS complexes of the virtual subjects with 0.84 ± 0.18 Pearson's correlation coefficient (mean ± standard deviation).
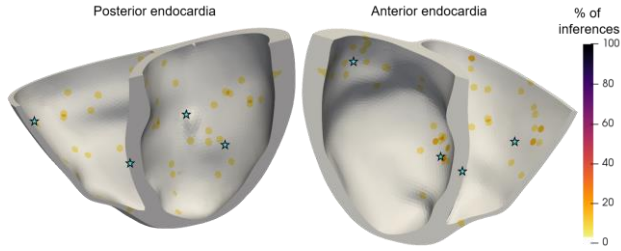

Figure 2. Root nodes inferred on virtual subjects with the Mesh-4 torso-biventricular anatomy. The stars indicate the ground-truth root node locations. The endocardial surface is coloured as a heatmap showing how often each location was inferred.

The inference of root nodes was more accurate on the anterior side of the heart than on the posterior (Figure 2) due to the left-anterior positioning of most electrodes in the 12-lead ECG test. The location errors for the root nodes across all twenty virtual subjects were 1.9 ± 0.5 cm and 1.7 ± 0.4 cm in the LV and RV, respectively. The analogous errors in the number of root nodes in the LV and in the RV were 0.6 ± 0.6 and 1.6 ± 0.8.
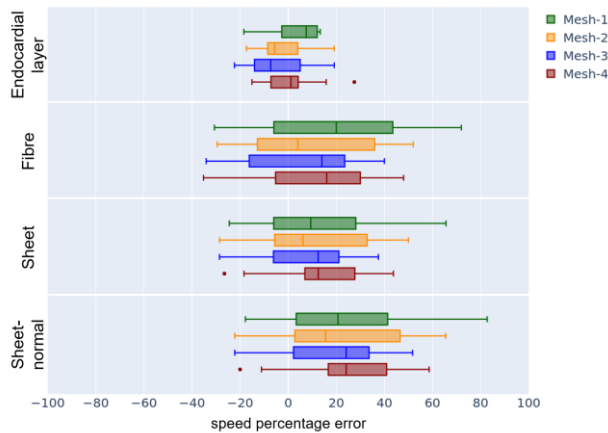

Figure 3. Error in the conduction speeds inference. The errors (x-axis) are computed as $error = 100 * (S' - S)/S$, where S' is the inferred conduction speed value, and S is the ground truth speed. They are represented as box plots grouped by anatomy (colour) and conduction speed (y-axis). The errors' absolute mean ± standard deviation across all anatomies were: 9.6 ± 6.2 – endocardial; 25.4 ± 16.0 – fibre; 20.5 ± 14.5 – sheet; and 27.7 ± 19.1 – normal.

The inference of the conduction speeds (Figure 3) demonstrated that the endocardial and sheet-directed speeds were recovered more accurately than the fibre and sheet-normal directed speeds. This finding suggests that the endocardial and sheet-directed speeds determined the activation wavefront's speed.

4.   Discussion

This study presents an inference method combined with CMR-based torso-biventricular Eikonal models to estimate the root nodes and conduction speeds from 12-lead ECGs. Our approach aims to serve as an efficient tool for generating cardiac 'digital twins', which is of paramount importance for precision cardiology. We conducted the simultaneous ECG-guided inference of endocardial, fibre, sheet, and sheet-normal conduction speeds and the location and number of the root nodes in the endocardium. Previous work provided inference for a limited number of properties. For example, in [16], the estimation was focused on locating two root nodes in the left ventricle and the conduction speeds from ECG data; whereas, in [9], the focus was on activation times of a known set of root nodes and the conduction speeds from epicardial activation maps.

Our inference method was successful at finding the ground truth conduction speeds (Figure 3) and root node locations (Figure 2) for a range of QRS complexes that represented the variability found in the healthy human population. The method was also shown to be robust to noise contamination.

Our results (Figure 2) suggest that the most critical parameters that affect the healthy ventricular sinus-rhythm activation sequence are the root nodes, the endocardial speed, and the sheet-directed speed, as these were better identified compared to the fibre and sheet-normal conduction speeds. This difference in the identifiability of the speeds was due to the relatively negligible impact of the fibre and sheet-normal speeds on the activation sequence since they act on the plane parallel to the endocardial layer and are dominated by the isotropic conduction pattern of the endocardium due to its faster conduction speed.

The root nodes were better recovered on the heart's anterior side (Figure 2). This was due to the predominantly anterior positioning of the standard precordial electrodes in the 12-lead ECG test, as the influence of a root node on an electrogram is inversely proportional to the distance between the cardiac region affected by the root node and the electrode's position.

Overall, this study presented the foundations of a novel pipeline capable of non-invasively calibrating cardiac digital twins for healthy subjects from synthetic 12-lead ECG recordings. Our approach was designed to easily accommodate disease conditions, such as pathological tissue heterogeneities (scars or fibrosis). We anticipate that

our methodology can be adapted to work with clinical ECG recordings from disease patients to generate cardiac digital twins in the clinic.

Acknowledgements

References

[1] S. A. Niederer, J. Lumens, and N. A. Trayanova, 'Computational models in cardiology', *Nat Rev Cardiol*, vol. 16, no. 2, pp. 100–111, Feb. 2019, doi: 10.1038/s41569-018-0104-y.

[2] P. M. Boyle *et al.*, 'Computationally guided personalized targeted ablation of persistent atrial fibrillation', *Nat Biomed Eng*, vol. 3, no. 11, pp. 870–879, Nov. 2019, doi: 10.1038/s41551-019-0437-9.

[3] J. Corral-Acero *et al.*, 'The "Digital Twin" to enable the vision of precision cardiology', *European Heart Journal*, p. ehaa159, Mar. 2020, doi: 10.1093/eurheartj/ehaa159.

[4] L. Cardone-Noott, A. Bueno-Orovio, A. Mincholé, N. Zemzemi, and B. Rodriguez, 'Human ventricular activation sequence and the simulation of the electrocardiographic QRS complex and its variability in healthy and intraventricular block conditions', *EP Europace*, vol. 18, no. suppl_4, pp. iv4–iv15, Dec. 2016, doi: 10.1093/europace/euw346.

[5] C. C. Drovandi and A. N. Pettitt, 'Estimation of Parameters for Macroparasite Population Evolution Using Approximate Bayesian Computation', *Biometrics*, vol. 67, no. 1, pp. 225–233, 2011, doi: 10.1111/j.1541-0420.2010.01410.x.

[6] A. Mincholé, E. Zacur, R. Ariga, V. Grau, and B. Rodriguez, 'MRI-Based Computational Torso/Biventricular Multiscale Models to Investigate the Impact of Anatomical Variability on the ECG QRS Complex', *Front. Physiol.*, vol. 10, 2019, doi: 10.3389/fphys.2019.01103.

[7] M. Wallman, N. P. Smith, and B. Rodriguez, 'A Comparative Study of Graph-Based, Eikonal, and Monodomain Simulations for the Estimation of Cardiac Activation Times', *IEEE Transactions on Biomedical Engineering*, vol. 59, no. 6, pp. 1739–1748, Jun. 2012, doi: 10.1109/TBME.2012.2193398.

[8] K. Gima and Y. Rudy, 'Ionic Current Basis of Electrocardiographic Waveforms: A Model Study', *Circulation Research*, vol. 90, no. 8, pp. 889–896, May 2002, doi: 10.1161/01.RES.0000016960.61087.86.

[9] T. Grandits *et al.*, 'An Inverse Eikonal Method for Identifying Ventricular Activation Sequences from Epicardial Activation Maps', *Journal of Computational Physics*, p. 109700, Jul. 2020, doi: 10.1016/j.jcp.2020.109700.

[10] D. D. Streeter, H. M. Spotnitz, D. P. Patel, J. Ross, and E. H. Sonnenblick, 'Fiber Orientation in the Canine Left Ventricle during Diastole and Systole', *Circulation Research*, vol. 24, no. 3, pp. 339–347, Mar. 1969, doi: 10.1161/01.RES.24.3.339.

[11] B. Caldwell, M. Trew, G. Sands, D. Hooks, I. LeGrice, and B. Smaill, 'Three Distinct Directions of Intramural Activation Reveal Nonuniform Side-to-Side Electrical Coupling of Ventricular Myocytes', *Circulation: Arrhythmia and Electrophysiology*, vol. 2, no. 4, pp. 433–440, Aug. 2009, doi: 10.1161/CIRCEP.108.830133.

[12] H. Sakoe and S. Chiba, 'Dynamic programming algorithm optimization for spoken word recognition', *IEEE Transactions on Acoustics, Speech, and Signal Processing*, vol. 26, no. 1, pp. 43–49, Feb. 1978, doi: 10.1109/TASSP.1978.1163055.

[13] F. Itakura, 'Minimum prediction residual principle applied to speech recognition', *IEEE Transactions on Acoustics, Speech, and Signal Processing*, vol. 23, no. 1, pp. 67–72, Feb. 1975, doi: 10.1109/TASSP.1975.1162641.

[14] D. Durrer, Van Dam R. Th., Freud G. E., Janse M. J., Meijler F. L., and Arzbaecher R. C., 'Total Excitation of the Isolated Human Heart', *Circulation*, vol. 41, no. 6, pp. 899–912, Jun. 1970, doi: 10.1161/01.CIR.41.6.899.

[15] Cerqueira Manuel D. *et al.*, 'Standardized Myocardial Segmentation and Nomenclature for Tomographic Imaging of the Heart', *Circulation*, vol. 105, no. 4, pp. 539–542, Jan. 2002, doi: 10.1161/hc0402.102975.

[16] S. Giffard-Roisin *et al.*, 'Sparse Bayesian Non-linear Regression for Multiple Onsets Estimation in Non-invasive Cardiac Electrophysiology', in *Functional Imaging and Modelling of the Heart*, Cham, 2017, pp. 230–238, doi: 10.1007/978-3-319-59448-4_22.

Addresses for correspondence:

Julia Camps
Department of Computer Science, University of Oxford, Wolfson building, Parks Road, Oxford, OX1 3QD, UK.
julia.camps@cs.ox.ac.uk